PARASUBICULAR EFFERENTS TO LAYER II OF THE ENTORHINAL CORTEX: MODULATION OF RESPONSES TO PIRIFORM CORTEX INPUTS *IN VIVO*

Douglas A. Caruana

A Thesis in

The Department of

Psychology

Presented in Partial Fulfillment of the Requirements

for the Degree of Master of Arts at Concordia University

Montréal, Québec

July, 2003.

Your file Votre référence
ISBN: 0-612-83815-3
Our file Notre référence
ISBN: 0-612-83815-3

ABSTRACT

Parasubicular Efferents to Layer II of the Entorhinal Cortex: Modulation of Responses to Piriform Cortex Inputs *In Vivo*

Douglas A. Caruana

Although a major output of the hippocampal formation is from the subiculum to the deep layers of the entorhinal cortex, the parasubiculum projects to the superficial layers of the entorhinal cortex, and may therefore modulate how the entorhinal cortex responds to sensory inputs from other cortical regions. Recordings at multiple depths in the entorhinal cortex were first used to characterize field potentials evoked by stimulation of the parasubiculum in urethane-anesthetized rats. Current source density analysis showed that a prominent surface-negative field potential component is generated by synaptic activation in layer II. The surface-negative field potential was also observed in rats with chronically implanted electrodes. The response was maintained during short stimulation trains of up to 125 Hz, suggesting that it is generated by activation of monosynaptic inputs to the entorhinal cortex. The piriform cortex also projects to layer II of the entorhinal cortex, and interactions between parasubicular and piriform cortex inputs were investigated using double-site stimulation tests. Simultaneous activation of parasubicular and piriform cortex inputs with high-intensity pulses resulted in smaller synaptic potentials than were expected on the basis of summing the individual responses, consistent with the termination of both pathways onto a common population of neurons. Paired-pulse tests were then used to assess the effect of parasubicular stimulation on responses to piriform cortex stimulation. Responses of the entorhinal cortex to piriform cortex inputs were inhibited when the parasubiculum was stimulated 5 ms earlier, and

were enhanced when the parasubiculum was stimulated 20 to 150 ms earlier. These results indicate that excitatory inputs to the entorhinal cortex from the parasubiculum may enhance the propagation of neuronal activation patterns into the hippocampal circuit by increasing the responsiveness of the entorhinal cortex to appropriately timed inputs.

ACKNOWLEDGEMENTS

I would like to thank Dr. C. Andrew Chapman for his patience, encouragement, and support during this project. I would also like to thank Dr. Saïd Kourrich and Dr. Bassam Hamam for many useful discussions regarding the entorhinal cortex. To my committee members, Dr. Barbara Woodside and Dr. David Mumby, thank you for your comments and feedback on an earlier draft of this manuscript. To everyone else who listened to me talk *ad infinitium* about my work: THANKS! The research conducted for this thesis was supported by grants to C.A. Chapman from the Natural Sciences and Engineering Research Council of Canada, the Fonds pour la Formation de Chercheurs et l'Aide á la Recherche, and the Canadian Foundation for Innovation.

TABLE OF CONTENTS

LIST OF FIGURES

LIST OF ABBREVIATIONS

AMPA	amino-3-hydroxy-5-methyl-isoxazole-propinoic acid
CA	Cornu ammonis
CC	Corpus callosum
CSD	Current source density
DG	Dentate gyrus
fEPSP	Field excitatory postsynaptic potential
GABA	Gamma aminobutyric acid
I_h	Hyperpolarization-activated non-specific cationic current
I/O	Input/output
i.p.	Intraperitoneal
IPSP	Inhibitory postsynaptic potential
LEC	Lateral entorhinal cortex
LD	Lamina dissecans
MEC	Medial entorhinal cortex
Mg^{2+}	Magnesium
N-K	Newman Keuls
NMDA	N-methyl-D-aspartate
PaS	Parasubiculum
PIR	Piriform cortex
PrS	Presubiculum
REM	Rapid eye movement

S	Subiculum
V2	Secondary visual cortex

INTRODUCTION

Multi-modal sensory information carried by inputs from the piriform, perirhinal, and postrhinal cortices (Amaral & Witter, 1995; Burwell & Amaral, 1998) converges within the superficial layers of the entorhinal cortex. Neurons in layer II of the entorhinal cortex, in turn, provide the hippocampus with the majority of its cortical sensory input through the perforant path projection to the dentate gyrus and CA3 region, and a smaller projection from layer III reaches the CA1 region and subiculum (Amaral & Witter, 1995; Witter, Groenewegen, Lopes da Silva, & Lohman, 1989). The factors which govern synaptic integration and temporal firing patterns in entorhinal cortex projection neurons are therefore likely to contribute to the information processing and mnemonic functions of the hippocampal formation.

The hippocampus and surrounding parahippocampal cortices have been investigated extensively with respect to their roles in learning and memory. While the hippocampus proper is thought to contribute preferentially to spatial memory (O'Keefe & Nadel, 1978; Squire, 1992), nearby parahippocampal cortices are thought to contribute differentially to other forms of information and mnemonic processing as well. Most notably, the perirhinal cortex has been found to play a critical role in object recognition memory as demonstrated by lesion studies in both rodents (Mumby & Glenn, 2000; Mumby, Glenn, Nesbitt, & Kyriazis, 2002; Mumby and Pinel, 1994) and primates (Buckley, Booth, Rolls, & Gaffen, 2001; Buckley & Gaffen, 1998). However, the close proximity that the entorhinal cortex has to the hippocampus, and the dense interconnectivity that the two structures share make it difficult to dissociate the individual contributions of either to learning and memory. Although lesions to extrahippocampal

cortices including the entorhinal cortex can cause pronounced spatial memory deficits (Glasier, Janis, Roof, & Stein, 1999; Hampson, Jarrard, & Deadwyler, 1999), more specific damage restricted to the entorhinal cortex itself results mainly in non-spatial memory impairments (Bannerman et al., 2001; Galani, Weiss, Cassel, & Kelche, 1998).

A common view regarding the primary function of the entorhinal cortex is that it serves as a cortical relay for sensory afferents intended for hippocampal processing (Amaral & Witter, 1995; Burwell & Amaral, 1998). Recent demonstrations of bi-directional plasticity in the superficial layers of the entorhinal cortex (Bouras & Chapman, 2003; Kourrich & Chapman, 2003) suggest that it may play a potential role in binding individual sensory elements together into cohesive representations prior to being relayed to the dentate gyrus and hippocampus. What is less known, however, are factors that may contribute to the modulation of physiological mechanisms responsible for such integrative functions. Both hippocampal and subcortical inputs to the superficial layers of the entorhinal cortex are thought to be relevant to this.

The medial septum sends a large cholinergic projection to the superficial layers of the entorhinal cortex (Alonso & Köhler, 1984; Gaykema, Luiten, Nyakas, & Traber, 1990). In rats, the importance of cholinergic inputs to several temporal lobe structures has been linked to the generation of membrane oscillations at theta frequency (4 to 12 Hz) within principal neurons during exploratory behaviours and REM sleep (see Buzsáki, 2002 for a review). Such rhythmic oscillations are believed necessary for the spatio-temporal synchronization of discrete neuronal populations across different cortical brain regions. Moreover, electrical stimulation of the medial septum can modulate field potentials recorded in the superficial layers of the entorhinal cortex evoked by stimulation

of sensory afferents originating from the piriform (primary olfactory) cortex (Chapman & Racine, 1997a), and suggests that heterosynaptic interactions can powerfully affect the excitability of neurons in layer II of the entorhinal cortex.

The hippocampal CA1 region and the subiculum are well-known to project to the deep layers of the entorhinal cortex (Amaral, Dolorfo, & Alvarez-Royo, 1991; Amaral & Witter, 1995; Swanson & Cowan, 1977), but the presubiculum and parasubiculum target the superficial layers, and may therefore modulate the firing of entorhinal cortex projection neurons induced by extrahippocampal cortical afferents. The six-layered cytoarchitecture of the pre- and parasubiculum is similar to that of the entorhinal cortex rather than to that of the subiculum, and their projections to the superficial layers of the entorhinal cortex further suggest that they be regarded as cortical structures mediating the input, rather than the output, of the hippocampal formation (Amaral & Witter, 1995; O'Mara, Commins, Anderson, & Grigg, 2001). Lesions confined to the pre- and parasubiculum have been shown to result in profound spatial memory deficits in rodents (Liu, Jarrard, & Bilkey, 2001), and demonstrate that these structures play an important role in mnemonic processing. The parasubicular projection to the entorhinal cortex, however, has received relatively little attention, and the physiological and functional role of this component of the circuitry of the hippocampal formation is poorly understood.

The presubiculum projects to layers I and III of the medial entorhinal cortex, with the majority of synaptic contacts on dendrites of layer III neurons (Caballero-Bleda & Witter, 1994; Köhler, 1984; van Groen & Wyss, 1990). The parasubiculum, however, targets layer II of both the medial and lateral entorhinal cortex (Caballero-Bleda & Witter, 1993, 1994; Köhler, 1985; van Groen & Wyss, 1990), and is therefore well-

poised to affect the firing of neurons of the perforant path. The parasubiculum receives inputs from the CA1 region and subiculum (Köhler, 1985; van Groen & Wyss, 1990), the laterodorsal, anteroventral, and anterodorsal thalamic nuclei (Shibata, 1993; van Groen & Wyss, 1992, 1995) and the basolateral amygdala (van Groen & Wyss, 1990). The manner in which the parasubiculum modulates entorhinal cortex responses to sensory inputs may therefore depend on afferents from subcortical structures, as well as on changes in activity within the hippocampal formation.

Although excitatory projections from the parasubiculum to the entorhinal cortex provide an intriguing pathway for the re-entrance of activity back into the hippocampal circuit, the superficial layers of the entorhinal cortex are dominated by high levels of inhibition (Funahashi & Stewart, 1998; Jones, 1993, 1995), and strong inhibitory responses have been observed in the few studies that have characterized parasubicular inputs to layer II electrophysiologically. Both AMPA and NMDA receptor-mediated EPSPs are evoked in layer II neurons following stimulation of the parasubiculum *in vitro* (Jones, 1990), but local inhibitory interneurons are also activated (Jones & Buhl, 1993), and synaptic responses in principal neurons are predominantly inhibitory (Jones, 1990). Stimulation of various sites within the hippocampus, subicular complex, and amygdala *in vivo* also evokes strong inhibitory responses in layer II cells (Colino & Fernandes de Molina, 1986; Finch & Babb, 1980; Finch, Tan, & Isokawa-Akesson, 1988; Finch, Wong, Derian, & Babb, 1986). It is therefore not known if parasubicular inputs to the entorhinal cortex promote or inhibit entorhinal cortex responses to extrahippocampal cortical afferents.

The present study used field potential recording techniques to characterize synaptic responses evoked by parasubicular inputs to the layer II of the medial entorhinal cortex in awake, adult rats, and to examine the role of the parasubiculum in modulating synaptic responses evoked by the large input from the piriform cortex (Burwell & Amaral, 1998; Chapman & Racine, 1997a,b; Chapman, Xu, Haykin, & Racine, 1998). Because field potentials generated by this pathway have not been reported previously, current source density analysis in acute preparations was used to determine the synaptic origins of field potential responses in layer II of the entorhinal cortex. Tests conducted in awake, freely-behaving animals indicate that the response is generated monosynaptically, and suggest that both the parasubiculum and piriform cortex target a common population of layer II neurons. Paired-pulse stimulation was then used to determine the time-courses of inhibitory and facilitatory mechanisms evoked by parasubicular stimulation, and to characterize the effect of parasubicular stimulation on responses of the entorhinal cortex to subsequent activation of the piriform cortex.

MATERIALS AND METHODS

Acute Recordings and CSD Analysis

Surgery. Male Long-Evans hooded rats (350 to 450 g; n = 10) were anesthetized with urethane (1.5 g/kg, i.p.) and placed in a Kopf stereotaxic apparatus with bregma and lambda leveled within 200 μm along the horizontal plane. Temperature was monitored with a rectal thermometer and maintained between 36.0 and 37.0°C using a regulated heating pad (Fine Science Tools, Model 21061) and/or heating lamp. A bipolar stimulating electrode made from Teflon-coated stainless-steel wire (125 μm exposed tips separated by 0.8 mm) was lowered through a burr hole into the right parasubiculum (P, 8.1 mm; L, 3.8 mm; V, 5.0 mm relative to bregma). Monopolar field potential recordings were obtained using a Tungsten electrode (50 to 80 μm tip diameter) placed in an oil-hydraulic micromanipulator (Narishige, MO-10). The recording electrode was held at an angle 40° above horizontal so that it could be advanced on a plane near-perpendicular to the surface of the entorhinal cortex. A small window was excised in the skull and the recording electrode was lowered slowly toward the ventral surface of the entorhinal cortex using coordinates 8.5 mm posterior and 4.8 mm lateral to bregma, and 4.2 mm dorsal to the interaural line. Coordinates were chosen based on the distribution of efferents from the parasubiculum to the entorhinal cortex in the rat (Caballero-Bleda & Witter, 1993). Warmed mineral oil was applied to the exposed dura. The stereotaxic apparatus was grounded and a stainless-steel jeweler's screw in the left frontal bone served as a reference electrode.

Depth Profile Recordings. The amplitude of evoked responses was maximized by placing the recording electrode in the superficial layers of the entorhinal cortex ≈200 μm

from the cortical surface, and by adjusting the vertical position of the stimulating electrode to minimize current thresholds. Electrical stimuli were generated with either a pulse generator (AMPI, Master 8) or a computer digital-to-analog channel (50 kHz), and a stimulus isolation unit (A-M Systems, Model 2200) was used to deliver 0.1 ms biphasic constant current square-wave pulses to the parasubiculum. Evoked field potentials were analog filtered (0.1 Hz to 5 kHz passband), amplified (A-M Systems, Model 1700), and digitized at 10 or 20 kHz (16 bit) for storage on computer hard disk using the software package Experimenter's Workbench (Datawave Tech.). A 30-minute baseline period preceded experimental testing, and pulse intensity was then set to evoke responses that were approximately 75% of maximal levels (300 to 800 μA) for subsequent recordings.

In order to localize synaptic currents that generate evoked responses, field potential recordings for current source density analysis were obtained at multiple depths in the entorhinal cortex. Responses were evoked by paired-pulse stimulation of the parasubiculum, and were recorded at 31 depths as the recording electrode was retracted from the cortical surface in 50 μm steps. Preliminary experiments demonstrated a strong facilitation using a 40 ms interpulse interval, and paired-pulse stimulation at this interval was used to better visualize responses. Ten responses were recorded at each depth using an inter-trial interval of 10 sec and then averaged.

Moving Stimulation Electrode. To determine if activation of structures close to the parasubiculum might contribute to response components, in some experiments the recording electrode was placed near layer II, and the location of the stimulating electrode was varied in 200 μm steps between 2 mm dorsal and 2 mm ventral to target coordinates.

Ten responses were recorded and averaged at each depth using an inter-trial interval of 10 sec.

Histology. Following electrophysiological recordings, cathodal current (100 μA) was passed through both electrodes to mark tip locations. Animals were perfused intracardially with 0.9% saline followed by 10% formalin. Brains were stored in 10% formalin and transferred to a 20% sucrose solution one day prior to sectioning. Saggital sections (40 μm) were stained with formal-thionin and digital photographs of sections containing electrode tracks were taken. Multiple recordings were sometimes obtained from the surface of the entorhinal cortex in cases when the electrode was advanced too far (typically ≈50 to 150 μm), and traces were removed from current source density analysis on the basis of locations of electrolytic lesions. Measures of laminar thicknesses were determined using the software package Scion Image (Scion Corp.) following the conventions of Amaral and Witter (1995). Tissue obtained from animals with chronic electrodes (below) was processed in the same manner.

Current Source Density Analysis. In order to localize the synaptic currents underlying field potentials evoked by parasubicular stimulation, current source density (CSD) analysis was performed on depth profile recordings. Field potentials result from the net movement of currents into and out of extracellular space. The activation of excitatory synapses generates an active current sink in extracellular space which, in turn, can generate a passive current source located nearby (Mitzdorf, 1985). Provided that principal cells within a restricted cortical lamina are activated in a homogeneous manner, extracellular current flows mainly in the direction perpendicular to the laminar plane (Mitzdorf, 1985; Vida, Czopf, & Czéh, 1995). According to Ohm's law, the amount of

current flow is proportional to strength of the voltage (ϕ) gradient, and depth profile recordings of field potentials at multiple depths through the cortex (i.e., the z axis) quantify the voltage gradient at each point in time ($\partial\phi/\partial_z$). Changes in the slope of the voltage gradient reflect changes in the amount of current flowing, and are due to membrane currents (I_m) such as those evoked by synaptic activation (Mitzdorf, 1985). The one dimensional CSD can be computed by:

$$-I_m = \sigma_z \cdot \partial^2\phi/\partial_z^2$$

where z is the plane perpendicular to the cortical laminae from which the depth profile was sampled and σ_z is the conductivity of extracellular space. Variations in the conductivity of extracellular space are typically assumed to have minimal effects on the results of CSD analysis (Mitzdorf, 1985), and the second derivative of the potential gradient ($\partial^2\phi/\partial_z^2$) can therefore be used to estimate CSD in arbitrary units. This was implemented by differentiating a seventh-degree polynomial interpolated through data points. Because the second derivative is strongly affected by high-frequency noise, depth profiles were digitally smoothed prior to calculating the second derivative using a Blackman window which removed components with periods less than 200 μm.

Chronic Recordings

Surgery. Male Long-Evans hooded rats (300 to 350 g; n = 11) were anesthetized with sodium pentobarbital (65 mg/kg, i.p.) and placed in a stereotaxic apparatus with bregma and lambda leveled. Bipolar stimulating electrodes (tip separation of 0.6 mm) were lowered through burr holes into the right piriform cortex (P, 3.6 mm; L, 6.5 mm; V, 9.0 mm relative to bregma) and parasubiculum (P, 8.1 mm; L, 3.8 mm; V, 5.0 mm). A Teflon-coated stainless-steel recording electrode (125 μm exposed tip) was advanced

into the superficial layers of the right entorhinal cortex (P 8.5 mm and L 4.8 mm relative to bregma, and 4.2 mm dorsal to the interaural line) at an angle 40° above horizontal. In three cases, the recording electrode was lowered vertically to the same coordinates. Vertical placements of stimulating electrodes were adjusted to minimize current thresholds, and the position of the recording electrode was adjusted to maximize response amplitudes. A stainless-steel jeweler's screw in the contralateral frontal bone served as a reference electrode, and a second screw in the left parietal bone served as ground. Electrode leads were connected to gold-plated Amphenol pins and mounted in a plastic 9-pin connector. The entire assembly was embedded in dental cement and anchored to the skull with stainless-steel jeweler's screws. Animals were housed individually and were tested after a ≥10 day recovery period during the lights-on phase of a 12-hour light-dark schedule.

Stimulation and Recording. Animals were placed in a 40 x 40 x 60 cm Plexiglas chamber surrounded by a Faraday cage, and recordings were obtained after animals had habituated and were in a quiet, resting state. Stability of responses was assessed using input/output tests conducted every 2 days over a 5 day period. During each input/output test, 10 responses to stimulation of either the parasubiculum or piriform cortex were recorded and averaged at each of 10 intensities (100 to 1000 μA) using a 10 sec inter-trial interval.

To determine if evoked responses are likely activated monosynaptically or polysynaptically, frequency of following tests were conducted in which short ≈100 ms-duration trains of pulses at frequencies ranging from 60 to 125 Hz were delivered to the parasubiculum at an intensity that evoked single-pulse responses ≈75% of maximal

levels. Monosynaptic pathways typically follow stimulation frequencies near 100 Hz while polysynaptic pathways tend to fail at frequencies less than 50 Hz due to variability in cell firing and summation of polysynaptic potentials (see Berry & Pentreath, 1976). Five trains were delivered at each frequency for averaging, and there was a 20 sec inter-trial interval.

To determine if piriform cortex and parasubicular inputs likely synapse onto overlapping populations of entorhinal cortex neurons, occlusion tests were used in which stimulation pulses delivered to both sites were timed to evoke simultaneous responses in the entorhinal cortex. With low-intensity pulses, simultaneous activation of either separate or overlapping populations of cells should result in responses that are equivalent to the summation of responses evoked by stimulating each input individually. In contrast, high-intensity pulses that cause much greater activation of the same population of neurons can result in an occlusion effect in which the response to combined stimulation is smaller than expected from summation (Chapman & Racine, 1997a). During these tests, pulse intensities were set to evoke either maximal responses, or responses that were ≈50% of maximal, and responses evoked by single-pulses were compared to responses evoked by combined stimulation. Due to differences in peak latencies of responses, the piriform cortex was stimulated 5.5 to 10 ms prior to the parasubiculum. Ten responses were recorded and averaged for each condition, and there was a 15 sec inter-trial interval.

Paired-pulse tests were used to assess the time-courses of short-term facilitation and inhibition effects in the entorhinal cortex evoked by parasubicular stimulation. In these tests, the effect of inhibitory and facilitatory mechanisms evoked by the first pulse

were assessed by monitoring changes in the response to the second pulse. Pairs of stimulation pulses, separated by interpulse intervals ranging from 5 to 1000 ms, were delivered to the parasubiculum using pulse intensities that evoked responses ≈75% of maximal. Fifteen responses were recorded for averaging at each interpulse interval, and there was a 10 sec inter-trial interval.

Double-site paired-pulse tests were used to determine if stimulation of the parasubiculum can modulate responses in the entorhinal cortex evoked by piriform cortex stimulation. A conditioning pulse was delivered to the parasubiculum prior to the delivery of a test-pulse to the piriform cortex at a variable delay interval (5 to 1000 ms). The conditioning pulse was set to evoke maximal responses, and the intensity of the test-pulse was set to evoke responses that were ≈75% of maximal. There was an inter-trial interval of 10 sec, and 15 responses were recorded for averaging at each interval. Amplitudes of responses to test-pulses were expressed as a percentage of amplitudes of responses to single-pulses delivered to the piriform cortex.

RESULTS

Acute Recordings

Histology. Synaptic field potential responses were evoked in the entorhinal cortex when the stimulating electrode was positioned in or near the parasubiculum (Figs. 1A, 2, and 3). Stimulation current may also have spread in some cases to activate low-threshold substrates in the caudal portion of the presubiculum, the corpus callosum, or deep layers of the entorhinal cortex. Recording electrode trajectories were nearly perpendicular to the laminar plane, and the overall thickness of the medial entorhinal cortex at these sites ranged from 1400 to 1660 μm.

Field Potential Depth Profiles. Stimulation of the parasubiculum evoked a similar pattern of field potentials in the entorhinal cortex in 7 of 10 animals. The main component of responses was a superficial negative deflection that peaked at depths between 250 and 400 μm below the surface, and which reversed in polarity at depths of 500 to 700 μm (Fig. 1A). The negative component had a mean onset latency of 3.9 ±1.1 ms, and a peak amplitude of 0.37 ±0.10 mV at a latency of 6.9 ±1.1 ms. The surface-negative component was preceded by one or two negative spike components with latencies near 2 to 4 ms. The spikes were maximal at depths of 50 to 650 μm, and reversed polarity in both deep and superficial sites in six animals. In four cases, a long-latency negative component, with onset and peak latencies of 10.8 ±1.7 and 21.0 ±1.2 ms, was also observed. This component was relatively small (0.10 ±0.03 mV), peaked at depths of 350 to 1350 μm, and showed no clear reversal. Paired-pulse stimulation caused a clear facilitation of the major surface-negative synaptic component in 5 of 7 animals

[133.9 ±17.8% of single-pulse levels for the group, $t(6) = 2.25$, $p = 0.07$], but did not enhance the spike or the small late negative component.

CSD Analysis. Current source density analysis showed that the major surface-negative component was generated by a current sink in layer II, and in one case the sink also included an adjacent portion of layer III. The current sink peaked in layer II at depths of 300 to 450 μm below the cortical surface at a mean latency of 6.6 ±1.4 ms. Adjacent current sources were located in layers I and III (Fig. 1B), and the layer III source sometimes bordered on, or included, the lamina dissecans (3 of 7 cases). Similar to results for the negative field potential component, paired-pulse stimulation caused a non-significant facilitation of the layer II current sink to 145.1 ±18.8% of single-pulse levels [$t(6) = 2.16$, $p = 0.07$].

The early spike components were associated with current sinks in layers II and III. In three cases, the sinks peaked at the layer II-III border, suggesting synchronous activation of layer II and III neurons, and the sinks were restricted to layer II in two cases, and to layer III in the remaining two cases. Corresponding current sources were located above and below the sinks at sites in layers I-II, and in layer III and the lamina dissecans.

The small, longer-latency deep-negative potential observed in four animals was associated with very long-lasting current sinks in layer III and/or V. All four rats displayed current sinks that peaked along the IV-V border at depths of 950 to 1100 μm, and in three cases a current sink was also observed in layer III (e.g., Fig. 1B).

In three additional animals, stimulation of sites outside of the parasubiculum (Fig. 2A, open squares; 2B, dashes lines) evoked field potentials that were not associated with

a layer II sink (data not shown). In one animal, stimulation near the presubiculum evoked an initial spike associated with a layer III sink, and a subsequent surface-negative synaptic potential associated with a layer III current sink that peaked at a latency of 3.8 ms, 750 μm below the cortical surface. In two animals, stimulation of sites ventral to the parasubiculum near the entorhinal cortex evoked deep-negative field potentials associated with layer III current sinks at latencies of 2.8 and 3.7 ms.

Moving Stimulation Electrode. To determine if stimulation of sites outside the parasubiculum may have contributed to the layer II sink, recordings in four animals were obtained while the position of the stimulating electrode was varied in 200 μm steps above and below target coordinates. The surface-negative component was activated most strongly when the stimulating electrode was in or near the parasubiculum (Fig. 3). Spike components were evoked by stimulation of sites within, and dorsal to, the parasubiculum, and an additional longer-latency spike (peak latency of ≈9 ms) was observed in three animals as the electrode passed into the corpus callosum. The long-latency spike was not observed in one animal that had dorsal stimulation sites in visual cortex.

Chronic Recordings.

Input/Output Tests. Field potentials evoked by stimulation of the parasubiculum in freely behaving rats were similar to those in acute recordings, and had a peak amplitude of 0.47 ±0.06 mV at a latency of 7.4 ±0.6 ms (Fig. 4A, n = 11). Field potentials evoked by piriform cortex stimulation were similar to those described previously (Bouras & Chapman, 2003; Chapman & Racine, 1997a), and contained a negative synaptic component with a peak amplitude of 0.36 ±0.04 mV at a latency of 16.9 ±0.5 ms (Fig. 4B). Current thresholds were 200 to 400 μA for the parasubiculum

and 100 to 400 μA for the piriform cortex, and responses increased linearly with stimulation intensity.

Frequency of Following Tests. To assess whether synaptic responses in the entorhinal cortex are likely generated monosynaptically, frequency of following tests were conducted. Responses to individual pulses during short stimulation trains at frequencies of 60 to 125 Hz were always clear at 60 Hz, but were less distinct as stimulation frequency was increased above 90 Hz (n = 7). Responses clearly failed at 70 Hz in two cases, and were maintained at frequencies between 80 and 125 Hz in the remaining animals (Fig. 5), consistent with a monosynaptic projection.

Occlusion Tests. Occlusion tests were conducted to assess whether inputs from the parasubiculum and piriform cortex likely synapse onto the same pool of neurons. Simultaneous activation of the entorhinal cortex with low-intensity pulses produced responses that were no different than expected from summing responses evoked by stimulation of either site alone (Fig. 6A). In contrast, simultaneous activation of the entorhinal cortex with high-intensity pulses resulted in responses that were significantly smaller than expected on the basis of summation [Fig. 6B; $F(3, 27) = 19.29$, $p < 0.01$; Newman-Keuls, $p < 0.01$; n = 10], suggesting that a ceiling effect limited the degree of activation of a common pool of entorhinal cortex neurons.

Paired-Pulse Tests. To assess the time-course of inhibitory and facilitatory mechanisms in the entorhinal cortex evoked by parasubicular stimulation, pairs of stimulation pulses were delivered to the parasubiculum separated by interpulse intervals ranging from 5 to 1000 ms (Fig. 7). Responses at the 10 ms interval were significantly inhibited to 34.3 ±23.9% of single-pulse levels [$F(14, 126) = 7.65$, $p < 0.001$; N-K, $p <$

0.001; n = 10]. The maximal paired-pulse facilitation of 188.3 ±34.4% was observed when the interpulse interval was 30 ms (N-K, $p < 0.001$) and responses returned to single-pulse levels at intervals greater than 40 ms.

Heterosynaptic inhibition and facilitation of piriform cortex responses by prior stimulation of the parasubiculum was assessed by delivering single conditioning pulses to the parasubiculum followed by delivery of test-pulses to the piriform cortex at variable delay intervals (Fig. 8). Responses to piriform cortex stimulation were significantly inhibited at the 5 ms interpulse interval to 62.2 ±17.0% of single-pulse levels [$F(14, 140) = 8.80$, $p < 0.001$; N-K, $p < 0.01$; n = 11] and were facilitated at interpulse intervals of 20 to 150 ms (163.1 ±19.4% at 20 ms). Activation of parasubicular inputs to the entorhinal cortex can therefore inhibit or facilitate subsequent synaptic responses to piriform cortex stimulation in a manner that depends on the timing of activation in the two pathways.

Figure 1. Evoked field potentials and the results of current source density analysis for a representative animal showing a surface-negative potential and an associated current sink in layer II of the entorhinal cortex following stimulation of the parasubiculum. **A**: Averaged field potentials recorded at multiple depths in the entorhinal cortex evoked by paired-pulse stimulation of the parasubiculum using a 40 ms interpulse interval. Note the major surface-negative field potential component that reverses ≈650 μm from the cortical surface, and the shorter-latency spike component at depths near 700 μm. **B**: Results of current source density analysis of responses in A (B_1) have been expanded to show the response to the first stimulation pulse more clearly (B_2). Results show that the short-latency spike is generated by a current sink located near the layer II-III border, and that the major synaptic component is generated by a current sink centered in layer II. Long latency and duration current sinks were also observed in layers III and V-VI in this animal. Dashed lines indicate borders between the cortical layers (LD: lamina dissecans). **C**: A single trace from A (arrow) has been expanded to show the various response components. Arrows highlight the stimulation artifacts; the filled circle indicates an early spike-like component; the filled square highlights a short-latency negative synaptic component; and the open circle indicates a long-latency negative synaptic component.

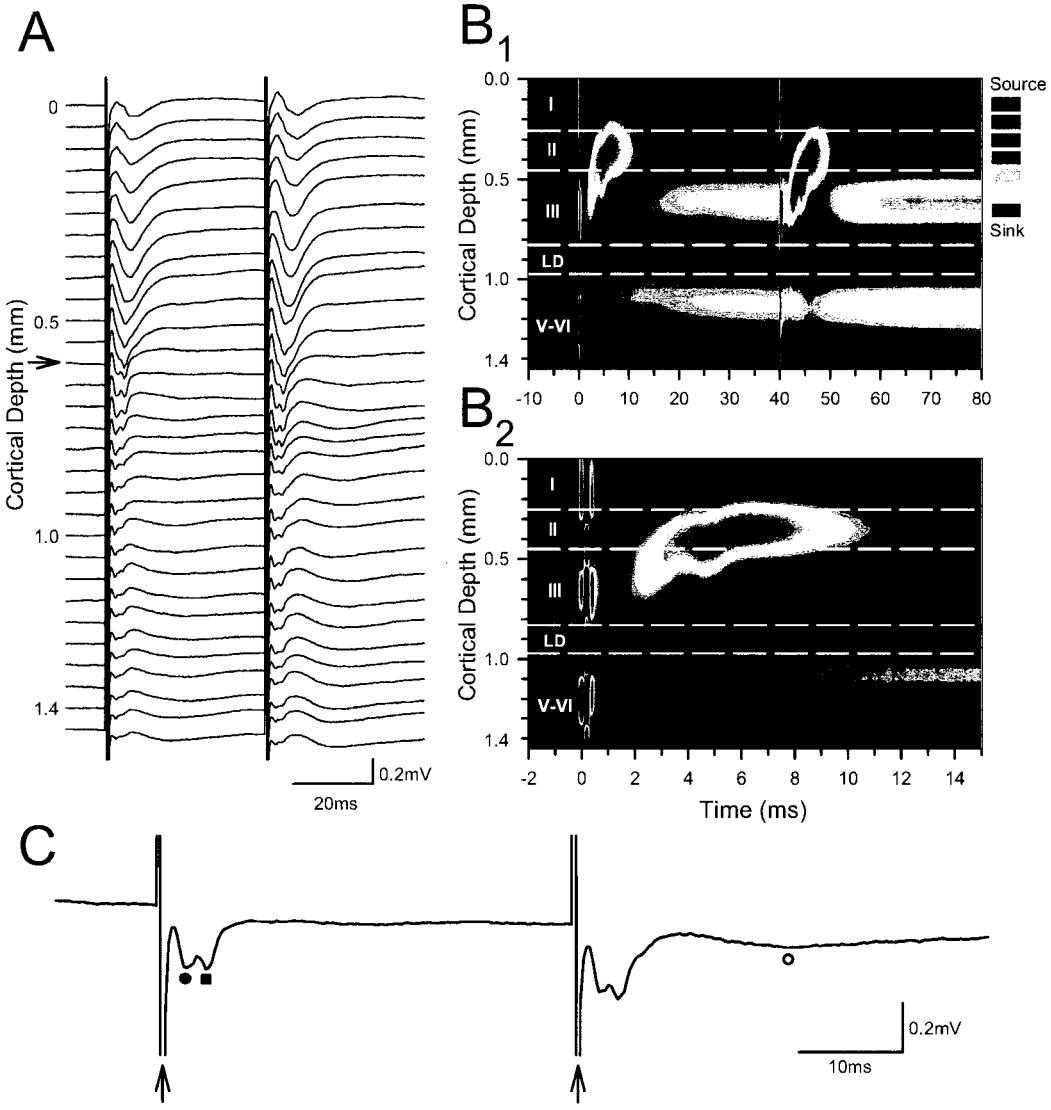
A
0
0.5
1.0
1.4
Cortical Depth (mm)
0.2mV
20ms
B1
0.0
0.5
1.0
1.4
Cortical Depth (mm)
I
II
III
LD
V-VI
-10
0
10
20
30
40
50
60
70
80
Source
Sink
B2
0.0
0.5
1.0
1.4
Cortical Depth (mm)
I
II
III
LD
V-VI
-2
0
2
4
6
8
10
12
14
Time (ms)
C
0.2mV
10ms

Figure 2. Histological results for CSD analysis experiments. **A and B:** Locations of the tips of the stimulating electrodes (A) and the recording electrode tracks (B) are shown on representative sections taken from the atlas of Paxinos and Watson (1998). Symbols in A, and lines in B, indicate positions of electrodes for the animal of Fig. 1 (open circle, bold line), other animals in which layer II sinks were observed (closed circles, solid lines), and animals in which layer II sinks were not observed (squares, dashed lines).

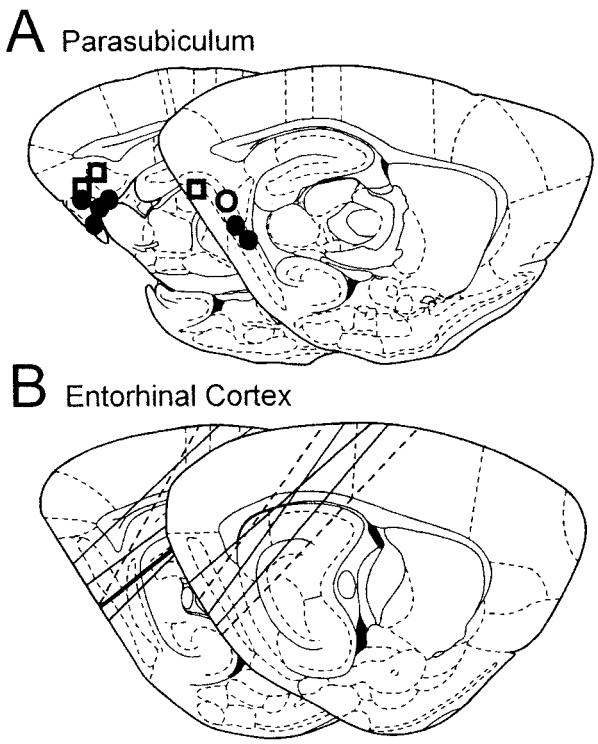
A Parasubiculum
B Entorhinal Cortex

Figure 3. **A**: Averaged field potentials recorded in layer II of the entorhinal cortex as the location of the stimulating electrode was varied in 200 μm steps. Numbers at left refer to the locations of the stimulating electrode shown in B. **B**: Stimulating electrode locations for the numbered traces in A are indicated by filled circles on a tracing of histological results. The major negative component of responses was evoked when the stimulating electrode was near the parasubiculum (PaS). Note the short-latency spike evoked at dorsal sites near the parasubiculum, and the long-latency spike evoked by stimulation near the corpus callosum (PrS: presubiculum; S: Subiculum; MEC: medial entorhinal cortex; LEC: lateral entorhinal cortex; V2: secondary visual cortex).

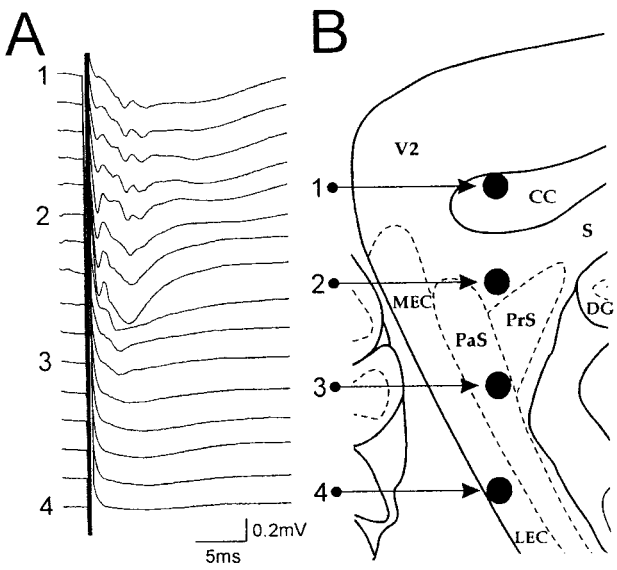
A
1
2
3
4
0.2mV
5ms
B
V2
CC
S
MEC
PrS
PaS
DG
LEC
1
2
3
4

Figure 4. **A** and **B**: Results of input/output tests following stimulation of the parasubiculum (A) and piriform cortex (B) in freely behaving animals. Representative field potentials in the entorhinal cortex are shown for the indicated pulse intensities (A_1, B_1) and mean peak amplitudes of responses are shown as a function of pulse intensity (A_2, B_2). Data indicate the mean ±1 SEM in this and subsequent figures.

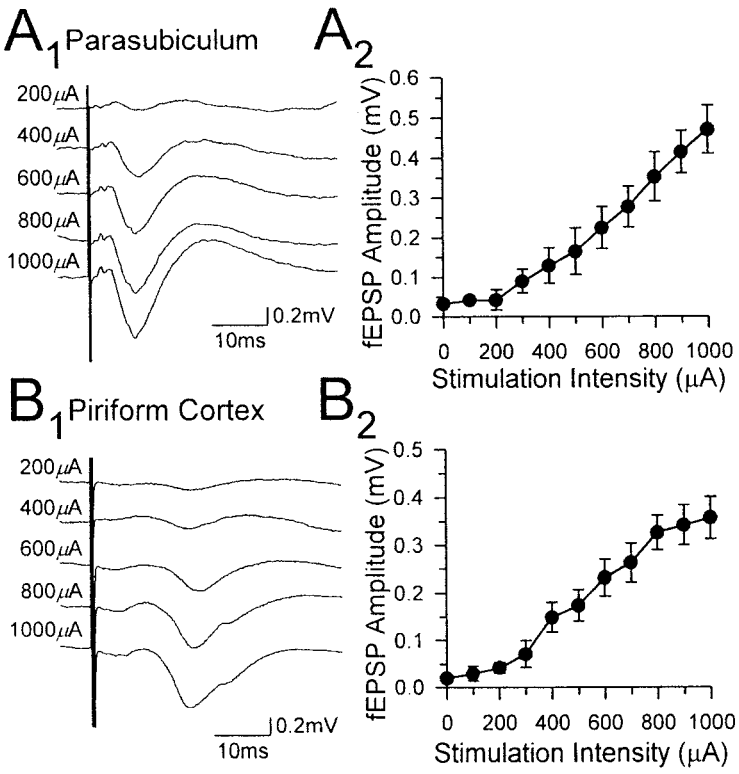
A1 Parasubiculum
200μA
400μA
600μA
800μA
1000μA
0.2mV
10ms
A2
fEPSP Amplitude (mV)
0.0
0.1
0.2
0.3
0.4
0.5
0.6
0
200
400
600
800
1000
Stimulation Intensity (μA)
B1 Piriform Cortex
200μA
400μA
600μA
800μA
1000μA
0.2mV
10ms
B2
fEPSP Amplitude (mV)
0.0
0.1
0.2
0.3
0.4
0.5
0
200
400
600
800
1000
Stimulation Intensity (μA)

Figure 5. Responses evoked in the entorhinal cortex by ≈100 ms-duration trains of pulses delivered to the parasubiculum at the indicated frequencies. Amplitudes of responses declined at higher stimulation frequencies, but individual responses to each pulse were maintained at frequencies near 100 Hz suggesting that responses are mediated by monosynaptic inputs from the parasubiculum.

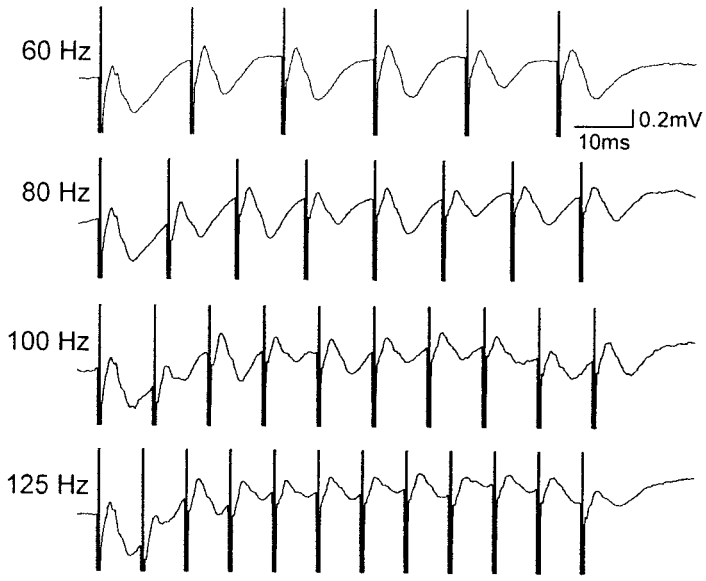
60 Hz
0.2mV
10ms
80 Hz
100 Hz
125 Hz

Figure 6. Results of occlusion tests in which stimulation of the parasubiculum (PaS) and piriform cortex (PIR) was timed to activate the entorhinal cortex simultaneously (PaS+PIR). **A**: Averaged responses evoked by stimulating each site alone using low-intensity pulses are compared to the response observed following combined stimulation (A_1, PaS+PIR, solid line), and the response expected from summing the individual responses (dashed line). There was no significant difference between the amplitudes of observed (Obs) and expected (Exp) responses for low-intensity pulses (A_2). **B**: Combined delivery of high-intensity pulses resulted in responses that were smaller than expected on the basis of summation. Conventions are as in A, and the arrow highlights the response expected from summation. The difference between observed and expected response amplitudes was significant only for high-intensity pulses (B_2; asterisk, $p < 0.01$), suggesting that parasubicular and piriform cortex efferents terminate on overlapping populations of entorhinal cortex neurons.

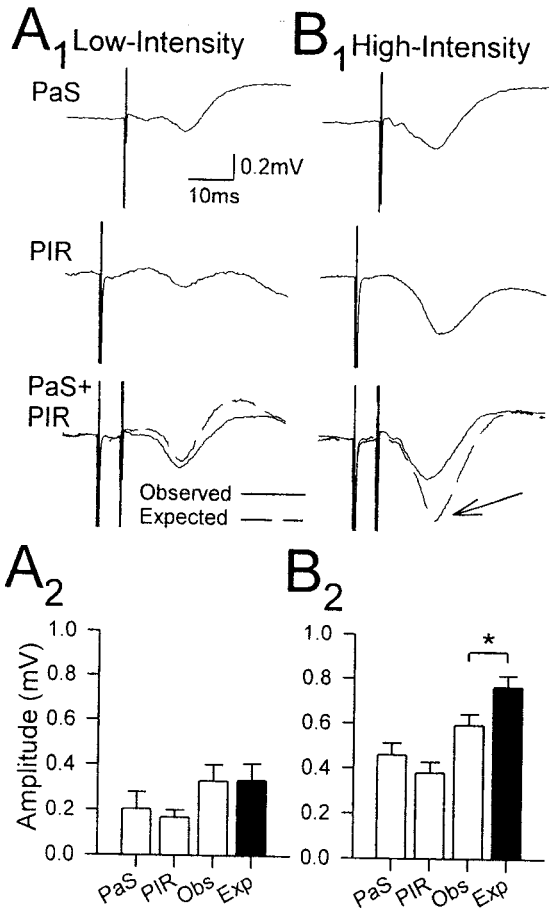
A1 Low-Intensity
B1 High-Intensity
PaS
0.2mV
10ms
PIR
PaS+
PIR
Observed
Expected
A2
B2
Amplitude (mV)
1.0
0.8
0.6
0.4
0.2
0.0
*
PaS
PIR
Obs
Exp

Figure 7. Paired-pulse stimulation of the parasubiculum caused inhibition of responses at the 10 ms interval, and facilitated responses at interpulse intervals of 30 and 40 ms. **A:** Representative averaged field potentials evoked by single-pulses and by pairs of pulses at intervals of 10, 30, and 1000 ms are shown. Note the absence of an observable response at the 10 ms interval (arrow) and the large facilitation of the response at the 30 ms interval. The dashed line indicates the mean amplitude of responses to single-pulses for comparison. **B:** Mean amplitudes of responses to second pulses are expressed as a percentage of amplitudes of responses evoked by the first pulse for each interpulse interval. Asterisks indicate significant differences from single-pulse levels (*, $p < 0.01$; **, $p < 0.001$).

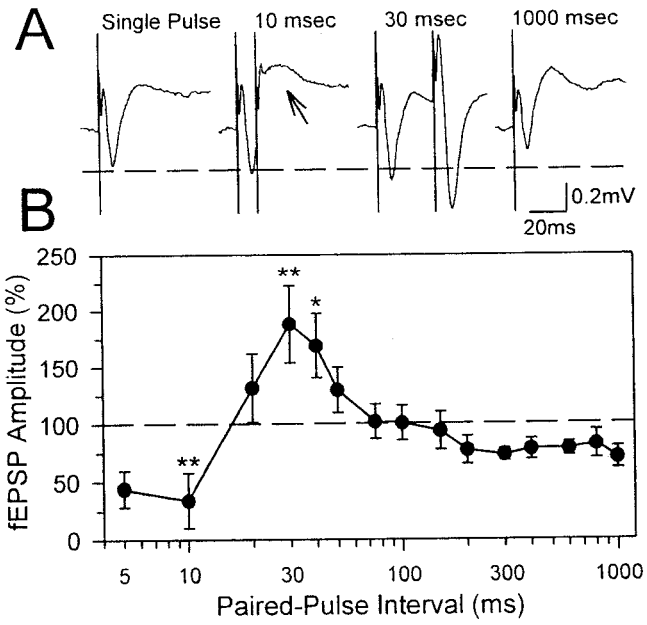
A
Single Pulse
10 msec
30 msec
1000 msec
0.2mV
20ms
B
fEPSP Amplitude (%)
250
200
150
100
50
0
**
**
*
5
10
30
100
300
1000
Paired-Pulse Interval (ms)

Figure 8. Delivery of a strong conditioning pulse to the parasubiculum causes a reduction in the amplitude of responses evoked by piriform cortex stimulation 5 ms later, but facilitates responses evoked by piriform cortex stimulation at longer delay intervals. **A:** Averaged field potentials evoked by single-pulses delivered to the piriform cortex, and by double-site paired-pulse stimulation at intervals of 5, 40, and 1000 ms are shown. The dashed line indicates the mean amplitude of responses evoked by single piriform cortex stimulation pulses. The size of the response evoked by piriform cortex stimulation was reduced (arrow) when the parasubiculum was stimulated 5 ms earlier, but was facilitated by stimulation of the parasubiculum at the 40 ms interpulse interval. **B:** Mean amplitudes of responses evoked by piriform cortex stimulation at various intervals following stimulation of the parasubiculum are expressed as a percentage of the amplitudes of responses evoked by single-pulses delivered to the piriform cortex. Responses were inhibited at the 10 ms interpulse interval, and were facilitated at intervals of 20 to 150 ms (*, $p < 0.05$; **, $p < 0.01$).

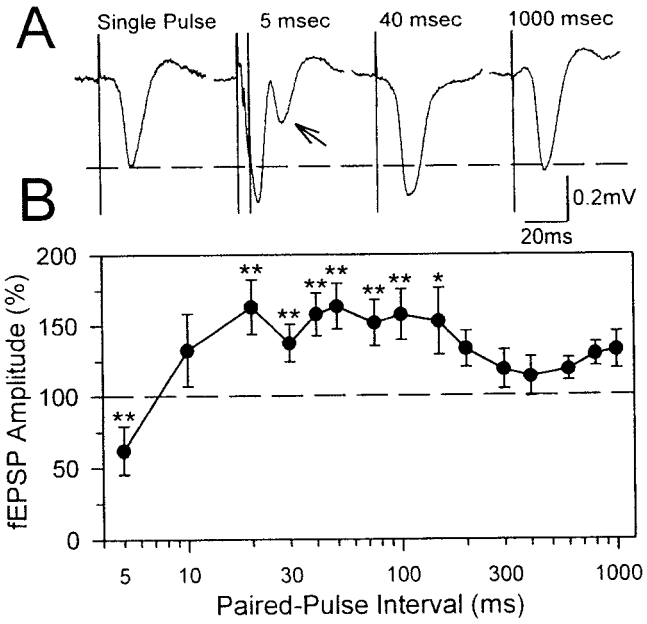
A
Single Pulse
5 msec
40 msec
1000 msec
B
0.2mV
20ms
fEPSP Amplitude (%)
200
150
100
50
0
5
10
30
100
300
1000
Paired-Pulse Interval (ms)

DISCUSSION

Field potential recording techniques have been used here to characterize parasubicular inputs to the entorhinal cortex in anesthetized and freely behaving rats, and to determine how this pathway modulates entorhinal cortex responses to inputs from the piriform cortex. Consistent with the direct projection from layer I and II of the parasubiculum to layer II of the entorhinal cortex (Caballero-Bleda & Witter, 1993; van Groen & Wyss, 1990), stimulation of the parasubiculum resulted in a monosynaptic surface-negative potential that is generated by inward synaptic currents in layer II (Figs. 1, 3, and 5). Stimulation of the parasubiculum resulted in the time-dependent inhibition or facilitation of inputs to the entorhinal cortex from the piriform cortex (Fig. 8), indicating that the parasubiculum may play a role in modulating the responsiveness of layer II of the entorhinal cortex to extrahippocampal cortical inputs. Further, inputs to the parasubiculum from area CA1 and the subiculum, and from amygdalar and thalamic nuclei (Köhler, 1985; van Groen & Wyss, 1990, 1992, 1995), provide routes through which ongoing activity in these structures can influence activity in entorhinal cortex projection neurons.

Current Source Density Analysis.

Field potentials in the entorhinal cortex evoked by stimulation of the parasubiculum in anesthetized animals contained a major surface-negative component, and one to two shorter-latency population spike-like components. Results of CSD analysis indicated that the major negative synaptic component was generated by a current sink in layer II, and that the early spikes were generated by current sinks in layer II and layer III. The synaptic component was most strongly activated when the stimulating

electrode was located in or near the parasubiculum (Fig. 3), and the inward currents observed in layer II are consistent with activation of excitatory afferents from the parasubiculum (Caballero-Bleda & Witter, 1993, 1994; Jones, 1990). The latency of the synaptic component is also consistent with the 4.2 ms onset latency of intracellular EPSPs evoked by stimulation of sites in the subicular complex (Finch et al., 1986).

The initial short-latency spike most likely reflects synchronous antidromic activation of entorhinal cortex layer II and/or III neurons by direct stimulation of the perforant path and/or temporoammonic path. Antidromic spikes in layer II and III neurons have also been recorded intracellularly at similar latencies following stimulation of the subicular complex and hippocampal formation *in vivo* (Finch et al., 1986, 1988). Short-latency spikes that sometimes followed the initial antidromic spike likely reflect synchronized firing resulting from both synaptic inputs and voltage-dependent conductances activated by the initial spike.

The initial spike appears to result from antidromic activation of entorhinal cortex neurons, but a resulting activation of recurrent collaterals between layer II neurons is unlikely to have contributed substantially to the synaptic response. Axon collaterals of layer II neurons can branch extensively (Dolorfo & Amaral, 1998; Klink & Alonso 1997), but recurrent connections between principal neurons in layer II appear to be rather sparse. Paired intracellular recordings have shown quite high probabilities of recurrent connections between layer III and layer V neurons in the rat, but have failed to find connections between layer II neurons (Dhillon & Jones, 2000; but see Biella, Uva, Hofmann, & de Curtis, 2002 in the guinea pig), and it has been suggested that many axonal arbourizations of layer II neurons target inhibitory cells (Dhillon & Jones, 2000).

Although the antidromic spike often involved substrates in layer III (5 of 7 cases), and recurrent collaterals are relatively common between layer III neurons (Dhillon & Jones, 2000), the synaptic component was associated with activation that included a portion of layer III in only one case. This suggests that the synaptic component is due primarily to monosynaptic activation of layer II neurons by parasubicular inputs, rather than being driven by activation of layer II or III axonal collaterals, or by monosynaptic inputs to layer III.

In four cases, weak deep-negative responses were associated with sinks in layers V and/or III, but the circuitry which mediates these long-latency, low-amplitude responses is not clear (e.g., Fig. 1). The long latencies and durations of these responses makes it unlikely that they were generated by direct activation of projections from the presubiculum, subiculum or CA1 region, but these pathways may have been driven polysynaptically by activation of the dentate gyrus, CA3, and/or subiculum (Witter et al., 1989).

Interactions Between Parasubicular and Piriform Cortex Inputs.

Field potentials in awake, freely-behaving rats were similar to those observed in anesthetized animals, and were used to assess interactions between inputs to the entorhinal cortex from the parasubiculum and piriform cortex. Stimulation of either input evoked field potential responses at the same recording site (Fig. 4), and results of occlusion tests were consistent with the termination of both input pathways on a common population of layer II neurons (Fig. 6). The occlusion of responses observed during simultaneous activation of entorhinal targets (Chapman & Racine, 1997a) might be explained partly by a non-linear increase in activation of feedforward inhibition by high-

intensity pulses, but field potentials in the medial entorhinal cortex following piriform cortex stimulation are known to result from activation in layer II (Chapman & Racine, 1997a), and peak latencies of inhibitory responses evoked by various inputs to the entorhinal cortex tend to be 5 to 10 ms longer than for EPSPs (Finch et al., 1986, 1988).

Paired-pulse tests assessed the time-course of inhibitory and facilitatory mechanisms evoked by parasubicular stimulation. At the shortest interpulse intervals, stimulation of the parasubiculum inhibited responses to both parasubicular and piriform cortex inputs (Figs. 7 and 8). The peak inhibition of parasubicular responses occurred at the 10 ms interpulse interval, and inhibition is observed at similar intervals following stimulation of the piriform cortex (Bouras & Chapman, 2003; Chapman & Racine, 1997a) and amygdala (Colino & Fernandes de Molina, 1986). Stimulation of the subicular complex *in vivo*, which included sites within the parasubiculum (Fig. $1_{M,K}$ in Finch et al., 1986), also evokes IPSPs in layer II neurons with a latency of about 10 ms (Finch et al., 1986, 1988). Stimulation of various sites in the hippocampal formation results in IPSPs in layer II cells with latencies that are strongly correlated with the latencies of EPSPs rather than with antidromic responses, suggesting that inhibitory responses are generated primarily by feedforward rather than by feedback inhibition (Finch et al., 1988). Stimulation of the parasubiculum *in vitro* activates inhibitory interneurons in layer II of the entorhinal cortex (Jones & Buhl, 1993) and results in prominent IPSPs in layer II principal cells (Jones, 1990) suggesting that the inhibition observed here may be mediated primarily by feedforward inhibition.

Feedforward inhibition also accounts for the heterosynaptic paired-pulse inhibition of responses to piriform cortex stimulation at the 5 ms interval (Finch et al.,

1988; Jones & Buhl, 1993). The interval at which maximal paired-pulse inhibition was observed was shorter for piriform cortex inputs than for parasubicular inputs (5 versus 10 ms), and this shorter interval corrects for the longer peak latency of piriform cortex evoked responses. Therefore, in both single- and double-site paired-pulses tests, the maximal inhibition was observed when test-responses occurred about 10 ms after the conditioning pulse.

At longer interpulse intervals, there was a facilitation of responses to both parasubicular and piriform cortex stimulation. Reasons for the shorter time-course of facilitation of parasubicular responses versus piriform cortex responses are not clear, but the heterosynaptic facilitation effect is similar to that observed in piriform cortex inputs following stimulation of the medial septum (Chapman & Racine, 1997a), and a prominent facilitation at intervals of 30 and 40 ms is also observed following paired-pulse stimulation of the piriform cortex (Bouras & Chapman, 2003; Chapman & Racine, 1997a). Homosynaptic paired-pulse facilitation is often attributed to enhanced transmitter release due to residual presynaptic calcium (Zucker, 1989), but this cannot explain heterosynaptic facilitation effects, and a number of additional mechanisms likely contribute. Responses evoked by piriform cortex (Alonso, de Curtis, & Llinás, 1990; Kourrich & Chapman, 2003) and parasubicular inputs (Jones, 1990) contain NMDA receptor-mediated components that could be enhanced by depolarization-induced weakening of the Mg^{2+}-block on the NMDA receptor channel. Layer II stellate neurons could be depolarized in part by activation of the persistent sodium current (Magistretti, Ragsdale, & Alonso, 1999), but a rebound depolarization mediated by the hyperpolarization-activated non-specific cationic current I_h (Alonso & Klink, 1993;

Dickson et al., 2000b; Dickson, Magistretti, Shalinsky, Hamam, & Alonso, 2000c) is more likely to contribute at longer intervals after the decay of inhibition. This current is a major contributor to paired-pulse facilitation in the sensorimotor cortex at long interpulse intervals (Castro-Alamancos & Connors, 1996; Werk & Chapman, 2003).

Reduced inhibitory synaptic transmission is also likely to have contributed to the facilitation effects observed here. Inhibition in the entorhinal cortex is reduced during repetitive stimulation (Jones, 1993, 1995), and paired-pulse facilitation in the CA1 is mediated in part by reduced inhibition during the response to the second pulse (Davies & Collingridge, 1996; Leung & Fu, 1994). Paired-pulse facilitation in the neocortex also results partly from activation of presynaptic autoreceptors that reduce GABA release during the second response (Deisz & Prince, 1989; Metherate & Ashe, 1994).

Together, the effects of parasubicular stimulation observed here are consistent with the activation of local inhibitory interneurons that inhibit layer II principal cells (Finch et al., 1988; Funahashi & Stewart, 1998; Jones & Buhl, 1993; Jones, 1995), and the subsequent facilitation of responses evoked a short time later. The activation of entorhinal cortex projection neurons is therefore likely to be affected by the relative timing of inputs from the parasubiculum and other cortical regions.

Functional Significance.

Excitatory inputs from the parasubiculum to the entorhinal cortex provide a pathway through which part of the "output" of the hippocampal formation can re-enter the hippocampal circuit. Patterns of activity among parasubicular neurons can be shaped by inputs from the CA1 region and subiculum, and this provides a mechanism through which ongoing hippocampal processing can influence which entorhinal cortex projection

neurons are most active, and most responsive to sensory inputs. Similarly, the parasubiculum may also affect patterns of activation in the dentate gyrus through its smaller projection to the molecular layer (Köhler, 1985; Witter, Holtrop, & van de Loosdrecht, 1988).

An important remaining question is to what extent parasubicular inputs to the entorhinal cortex may affect long-term synaptic plasticity in layer II. Because of the facilitation observed in the double-site paired-pulse experiments (Fig. 8), parasubicular activation could enhance neuronal excitability and contribute to heterosynaptic long-term potentiation and depression effects in sensory inputs to the entorhinal cortex. Synaptic plasticity within the hippocampal formation is thought to contribute to the mnemonic processing of spatial information (Bliss & Collingridge, 1993), and parasubicular inputs to the entorhinal cortex could contribute to lasting plasticity in the entorhinal cortex that could be important for the encoding of specific sensory representations, as well as the modulation of sensory afferents received by the hippocampus.

The parasubicular input to the entorhinal cortex may also provide a specific pathway through which emotional aspects of information processing mediated by the amygdala can modulate mnemonic processing in the hippocampus. When an animal is threatened, for example, inputs from the amygdala may dominate afferent control of the parasubiculum and result in an enhancement of the salience or transmission of threat-relevant aspects of the situation from the entorhinal cortex through to the hippocampus.

The parasubiculum is more likely to affect activity in the entorhinal cortex during theta- and gamma-frequency activity than during hippocampal CA1 sharp-waves. Sharp-waves are associated with increased firing in deep layers of the subiculum, presubiculum,

parasubiculum, and entorhinal cortex (Chrobak & Buzsáki, 1994), but the parasubicular projection to the entorhinal cortex arises from layer II and III neurons (Funahashi & Stewart, 1997; van Groen & Wyss, 1990), and sharp-waves are not associated with increased firing in the superficial layers of the parasubiculum or entorhinal cortex (Chrobak & Buzsáki, 1994). The parasubiculum receives a prominent input from the medial septum (Alonso & Köhler, 1984; Gaykema et al., 1990), and Taube (1995) has observed that a substantial proportion of parasubicular cells (≈41%) fire in relation to theta, and often fire in rhythmic bursts. Gamma-frequency activity is generated in layer II of the entorhinal cortex by synchronous synaptic inputs during the negative phase of the theta rhythm (Chrobak & Buzsáki, 1998; Dickson, Biella, & de Curtis, 2000a), and maximal paired-pulse facilitation effects were observed at an interval similar to the period of the gamma rhythm (Fig. 7). Theta- and gamma-frequency activities in the entorhinal cortex may therefore be accompanied by inputs from the parasubiculum which may enhance the responsiveness of layer II neurons to cortical sensory inputs. This may affect the processing of olfactory information and could also contribute heterosynaptically to lasting changes in synaptic strength (Chapman & Racine, 1997b; Kourrich & Chapman, 2003).

REFERENCES

Alonso, A., de Curtis M., & Llinás, R. (1990). Postsynaptic Hebbian and non-Hebbian long-term potentiation of synaptic efficacy in the entorhinal cortex in slices and in the isolated adult guinea pig brain. *Proceedings of the National Academy of Sciences*, *87*, 9280-9284.

Alonso, A., & Köhler, C. (1984). A study of the reciprocal connections between the septum and the entorhinal area using anterograde and retrograde axonal transport methods in the rat brain. *Journal of Comparative Neurology*, *225*, 327-343.

Alonso, A., & Klink, R. (1993). Differential electroresponsiveness of stellate and pyramidal-like cells of medial entorhinal cortex layer II. *Journal of Neurophysiology*, *70*, 128-142.

Amaral, D.G., Dolorfo, C., & Alvarez-Royo, P. (1991). Organization of CA1 projections to the subiculum: A PHA-L analysis in the rat. *Hippocampus*, *1*, 415-435.

Amaral, D.G., & Witter, M.P. (1995). Hippocampal formation. In G. Paxinos (Ed), The rat nervous system, 2nd edition (pp. 443-494). San Diego: Academic Press.

Bannerman, D.M., Yee, B.K., Lemaire, M., Wilbrecht, L., Jarrard, L., Iversen, S.D., Rawlins, J.N., & Good, M.A. (2001). The role of the entorhinal cortex in two forms of spatial learning and memory. *Experimental Brain Research*, *141*, 281-303.

Berry, M.S., & Pentreath, V.W. (1976). Criteria for distinguishing between monosynaptic and polysynaptic transmission. *Brain Research*, *105*, 1-20.

Biella, G., Uva, L., Hofmann, U.G., & de Curtis, M. (2002). Associative interactions within the superficial layers of the entorhinal cortex of the guinea pig. *Journal of*

Neurophysiology, *88*, 1159-1165.

Bouras, R., & Chapman, C.A. (2003). Long-term synaptic depression in the adult entorhinal cortex *in vivo*. *Hippocampus* (in press).

Bliss, T.V.P., & Colingridge, G.L. (1993). A synaptic model of memory: Long-term potentiation in the hippocampus. *Nature*, *361*, 31-39.

Buckley, M.J., Booth, M.C., Rolls, E.T., & Gaffen, D. (2001). Selective perceptual impairments after perirhinal cortex ablation. *Journal of Neuroscience*, *21*, 9824-36.

Buckley, M.J., & Gaffan, D. (1998). Perirhinal cortex ablation impairs visual object identification. *Journal of Neuroscience*, *18*, 2268-75.

Burwell, R.D., & Amaral, D.G. (1998). Cortical afferents of the perirhinal, postrhinal and entorhinal cortices of the rat. *Journal of Comparative Neurology*, *398*, 179-205.

Buzsáki, G. (2002). Theta oscillations in the hippocampus. *Neuron*, *33*, 325-340.

Caballero-Bleda, M., & Witter, M.P. (1993). Regional and laminar organization of projections from the presubiculum and parasubiculum to the entorhinal cortex: An anterograde tracing study in the rat. *Journal of Comparative Neurology*, *328*, 115-129.

Caballero-Bleda, M., Witter, M.P. (1994). Projections form the presubiculum and the parasubiculum to morphologically characterized entorhinal-hippocampal projection neurons in the rat. *Experimental Brain Research*, *101*, 93-108.

Castro-Alamancos, M.A., & Connors, B.W. (1996). Cellular mechanisms of the augmenting response: Short-term plasticity in a thalamocortical pathway. *Journal of Neuroscience*, *16*, 7742-7756.

Chapman, C.A., & Racine, R.J. (1997a). Converging inputs to the entorhinal cortex from the piriform cortex and medial septum: Facilitation and current source density analysis. *Journal of Neurophysiology*, *78*, 2602-2615.

Chapman, C.A., & Racine, R.J. (1997b). Piriform cortex efferents to the entorhinal cortex *in vivo*: Kindling induced potentiation and the enhancement of long-term potentiation by low-frequency piriform cortex or medial septal stimulation. *Hippocampus*, *7*, 257-270.

Chapman, C.A., Xu, Y., Haykin, S., & Racine, R.J. (1998). Beta-frequency (15-35 Hz) electroencephalogram activities elicited by toluene and electrical stimulation in the behaving rat. *Neuroscience*, *86*, 1307-1319.

Chrobak, J.J., & Buzsáki, G. (1994). Selective activation of deep layer (V-VI) retrohippocampal cortical neurons during hippocampal sharp waves in the behaving rat. *Journal of Neuroscience*, *14*, 6160-6170.

Chrobak, J.J., & Buzsáki, G. (1998). Gamma oscillations in the entorhinal cortex of the freely behaving rat. *Journal of Neuroscience*, *18*, 388-398.

Colino, A., & Fernandez de Molina, A. (1986). Inhibitory response in entorhinal and subicular cortices after electrical stimulation of the lateral and basolateral amygdala of the rat. *Brain Research*, *378*, 416-419.

Davies, C.H., & Collingridge, G.L. (1996). Regulation of EPSPs by the synaptic activation of $GABA_B$ autoreceptors in rat hippocampus. *Journal of Physiology (London)*, *496*, 451-470.

Deisz, R.A., & Prince, D.A. (1989). Frequency-dependent depression of inhibition in guinea-pig neocortex *in vitro* by $GABA_B$ receptor feed-back on GABA release.

Journal of Physiology (London), *412*, 513-541.

Dhillon, A., & Jones, R.S.G. (2000). Laminar differences in recurrent excitatory transmission in the rat entorhinal cortex *in vitro*. *Neuroscience*, *99*, 413-422.

Dickson, C.T., Biella, G., & de Curtis, M. (2000a). Evidence for spatial modules mediated by temporal synchronization of carbachol-induced gamma rhythm in medial entorhinal cortex. *Journal of Neuroscience*, *20*, 7846-7854.

Dickson, C.T., Magistretti, J., Shalinsky, M.H., Fransen, E., Hasselmo, M.E., & Alonso, A. (2000b). Properties and role of I(h) in the pacing of subthreshold oscillations in entorhinal cortex layer II neurons. *Journal of Neurophysiology*, *83*, 2562-2579.

Dickson, C.T., Magistretti, J., Shalinsky, M., Hamam, B., & Alonso, A. (2000c). Oscillatory activity in entorhinal neurons and circuits. Mechanisms and function. *Annals of the New York Academy of Sciences*, *911*, 127-150.

Dolorfo, C.L., & Amaral, D.G. (1998). Entorhinal cortex of the rat: Organization of intrinsic connections. *Journal of Comparative Neurology*, *398*, 49-82.

Finch, D.M., & Babb, T.L. (1980). Inhibition in subicular and entorhinal principal neurons in response to electrical stimulation of the fornix and hippocampus. *Brain Research*, *196*, 89-98.

Finch, D.M., Wong, E.E., Derian, E.L., & Babb, T.L. (1986). Neurophysiology of limbic system pathways in the rat: Projections from the subicular complex and hippocampus to the entorhinal cortex. *Brain Research*, *397*, 205-213.

Finch, D.M., Tan, A.M., & Isokawa-Akesson M. (1988). Feedforward inhibition of the rat entorhinal cortex and subicular complex. *Journal of Neuroscience*, *8*, 2213-2226.

Funahashi, M., & Stewart, M. (1997). Presubicular and parasubicular cortical neurons of the rat: Electrophysiological and morphological properties. *Hippocampus*, *7*, 117-129.

Funahashi, M., Stewart, M. (1998). GABA receptor-mediated post-synaptic potentials in the retrohippocampal cortices: Regional, laminar and cellular comparisons. *Brain Research*, *787*, 19-33.

Galani, R., Weiss, I., Cassel, J.C., & Kelche, C. (1998). Spatial memory, habituation, and reactions to spatial and nonspatial changes in rats with selective lesions of the hippocampus, the entorhinal cortex or the subiculum. *Behavioural Brain Research*, *96*, 1-12.

Gaykema, R.P.A., Luiten, P.G.M., Nyakas, C., & Traber, J. (1990). Cortical projection patterns of the medial septum-diagonal band complex. *Journal of Comparative Neurology*, *293*, 103-124.

Glasier, M.M., Janis, L.S., Roof, R.L., & Stein, D.G. (1999). Effects of unilateral entorhinal cortex lesion on retention of water maze performance. *Neurobiology of Learning and Memory*, *71*, 19-33.

Hampson, R.E., Jarrard, L.E., & Deadwyler, S.A. (1999). Effects of ibotenate hippocampal and extrahippocampal destruction on delayed-match and -nonmatch-to-sample behavior in rats. *Journal of Neuroscience*, *19*, 1492-507.

Jones, R.S.G. (1990). Synaptic responses of neurones in layer II of the rat medial entorhinal cortex to stimulation of the para-subiculum *in vitro*. *Journal of Physiology (London)*, *426*, 48P.

Jones, R.S.G. (1993). Entorhinal-hippocampal connections: A speculative view of their

function. *Trends in Neurosciences*, *16*, 58-64.

Jones, R.S.G. (1995). Frequency-dependent alterations in synaptic transmission in entorhinal-hippocampal pathways. *Hippocampus*, *5*, 125-128.

Jones, R.S.G., & Buhl, E.H. (1993). Basket-like interneurones in layer II of the entorhinal cortex exhibit a powerful NMDA-mediated synaptic excitation. *Neuroscience Letters*, *149*, 35-39.

Klink, R., & Alonso, A. (1997). Morphological characteristics of layer II projection neurons in the rat medial entorhinal cortex. *Hippocampus*, *7*, 571-583.

Kourrich, S., & Chapman, C.A. (2003). NMDA receptor-dependent long-term synaptic depression in the entorhinal cortex *in vitro*. *Journal of Neurophysiology*, *89*, 2112-2119.

Köhler, C. (1984). Morphological details of the projection from the presubiculum to the entorhinal area as shown with the novel PHA-L immunohistochemical tracing method in the rat. *Neuroscience Letters*, *45*, 285-290.

Köhler, C. (1985). Intrinsic projections of the retrohippocampal region in the rat brain. I. The subicular complex. *Journal of Comparative Neurology*, *236*, 504-522.

Leung, L.S., & Fu, X.W. (1994). Factors affecting paired-pulse facilitation in hippocampal CA1 neurons *in vitro*. *Brain Research*, *650*, 75-84.

Liu, P., Jarrard, L.E., & Bilkey, D.K. (2001). Excitotoxic lesions of the pre- and parasubiculum disrupt object recognition and spatial memory processes. *Behavioral Neuroscience*, *115*, 112-24.

Magistretti, J., Ragsdale, D.S., & Alonso, A. (1999). High-conductance sustained single-channel activity responsible for the low-threshold persistent Na^+ current in

entorhinal cortex neurons. *Journal of Neuroscience*, *19*, 7334-7341.

Metherate, R., & Ashe, J.H. (1994). Faciliation of an NMDA receptor-mediated EPSP by paired-pulse stimulation in rat neocortex via depression of GABAergic IPSPs. *Journal of Physiology (London)*, *481*, 331-348.

Mitzdorf , U. (1985). Current source-density method and application in cat cerebral cortex: Investigation of evoked potentials and EEG phenomena. *Physiological Review*, *65*, 37-100.

Mumby, D.G., & Pinel, J.P. (1994). Rhinal cortex lesions and object recognition in rats. *Behavioral Neuroscience*, *108*, 11-8.

Mumby, D.G., & Glenn, M.J. (2000). Anterograde and retrograde memory for object discriminations and places in rats with perirhinal cortex lesions. *Behavioural Brain Research*, *114*, 119-34.

Mumby, D.G., Glenn, M.J., Nesbitt, C., & Kyriazis, D.A. (2002). Dissociation in retrograde memory for object discriminations and object recognition in rats with perirhinal cortex damage. *Behavioural Brain Research*, *132*, 215-26.

O'Keefe, J., & Nadel, L. (1978). *The hippocampus as a cognitive map*. London: Oxford University Press.

O'Mara, S.M., Commins, S., Anderson, M., & Grigg, J. (2001). The subiculum: A review of from, physiology and function. *Progress in Neurobiology*, *64*, 129-155.

Paxinos, G., & Watson, C. (1998). *The rat brain in stereotaxic coordinates, 4th edition.* San Diego: Academic Press.

Shibata, H. (1993). Direct projections from the anterior thalamic nuclei to the retrohippocampal region in the rat. *Journal of Comparative Neurology*, *337*, 431-

445.

Squire, L. (1992). Memory and the hippocampus: A synthesis from findings with rats, monkeys, and humans. *Psychological Review*, *99*, 195-231.

Swanson, L.W., & Cowan, W.M. (1977). An autoradiographic study of the organization of the efferent connections of the hippocampal formation in the rat. *Journal of Comparative Neurology*, *172*, 49-84.

Taube, J.S. (1995). Place cells recorded in the parasubiculum of freely moving rats. *Hippocampus*, *5*, 569-583.

van Groen, T., & Wyss, J.M. (1990). The connections of presubiculum and parasubiculum in the rat. *Brain Research*, *518*, 227-243.

van Groen, T., & Wyss, J.M. 1992. Projections from the laterodorsal nucleus of the thalamus to the limbic and visual cortices in the rat. *Journal of Comparative Neurology*, *324*, 427-448.

van Groen, T., & Wyss, J.M. (1995). Projections from the anterodorsal and anteroventral nucleus of the thalamus to the limbic cortex in the rat. *Journal of Comparative Neurology*, *358*, 584-604.

Vida, I., Czopf, J., & Czeh, G. (1995). A current-source density analysis of the long-term potentiation in the hippocampus. *Brain Research*, *671*, 1-11.

Werk, C.M., & Chapman, C.A. (2003). Long-term potentiation of polysynaptic responses in layer V of the sensorimotor cortex induced by theta-patterned tetanization in the awake rat. *Cerebral Cortex*, *13*, 500-507.

Witter, M.P., Groenewegen, H.J., Lopes da Silva, F.H., & Lohman, H.M. (1989). Functional organization of the extrinsic and intrinsic circuitry of the

parahippocampal region. *Progress in Neurobiology*, *33*, 161-253.

Witter, M.P., Holtrop, R., & van de Loosdrecht, A.A. (1988). Direct projections from the periallocortical subicular complex to the fascia dentata in the rat: An anatomical tracing study using *Phaseolus vulgaris* leucoagglutinin. *Neuroscience Research Communications*, *2*, 61-68.

Zucker, R.S. (1989). Short-term synaptic plasticity. *Annual Review of Neuroscience*, *12*, 13-31.